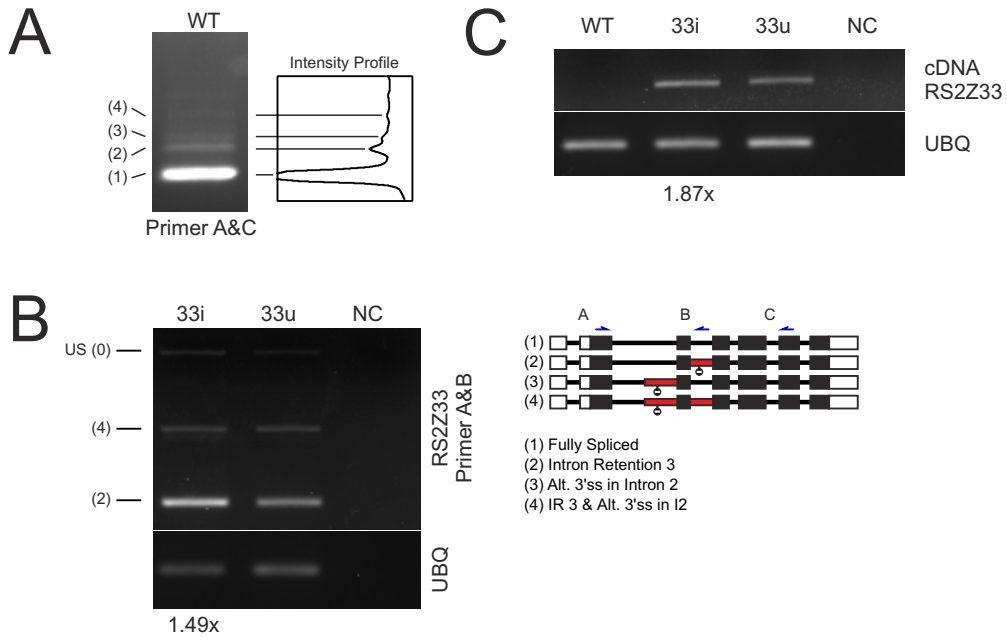

Supplemental Figure 1: Splice variants carrying intron retention 3 are upregulated in the induced RS2Z33 cell culture. A) Gel-separation of RT-PCR products of the RS2Z33 splice variants of untreated wildtype suspension cells with respective intensity profile (created with ImageJ). Splice variant 2 (intron retention 3) is the most abundant alternative splice variant in the cell suspension culture. B) Gel-separation of RT-PCR products of the RS2Z33 splice variants in fractionated cell extracts of induced and uninduced RS2Z33 inducible cell culture using an intron3-specific primer and one primer against exon 1. The induced population (33i) exhibits an upregulation of the intron 3 retaining transcript. WT - wildtype; 33i - induced RS2Z33 inducible suspension cell culture; 33u - uninduced population; NC - negative control (water); alt 3'ss in I2 & IR3 - transcripts carrying alternative 3' splice sites in intron 2 and a retained intron 3; US - unspliced transcript. Stop signs indicate the position of the PTCs. C) Gel-separation of RT-PCR product of RS2Z33 (At2g37340) using one vector-specific primer targeting the 35S minimal promoter and a primer specific to exon 4 of RS2Z33. Comparison of the wild type cell culture (col-0) and the beta-estradiol inducible cell culture with integrated RS2Z33-3'HA (full CDS). The induced cell population shows higher expression of the transgene than the uninduced population (33i vs. 33u).

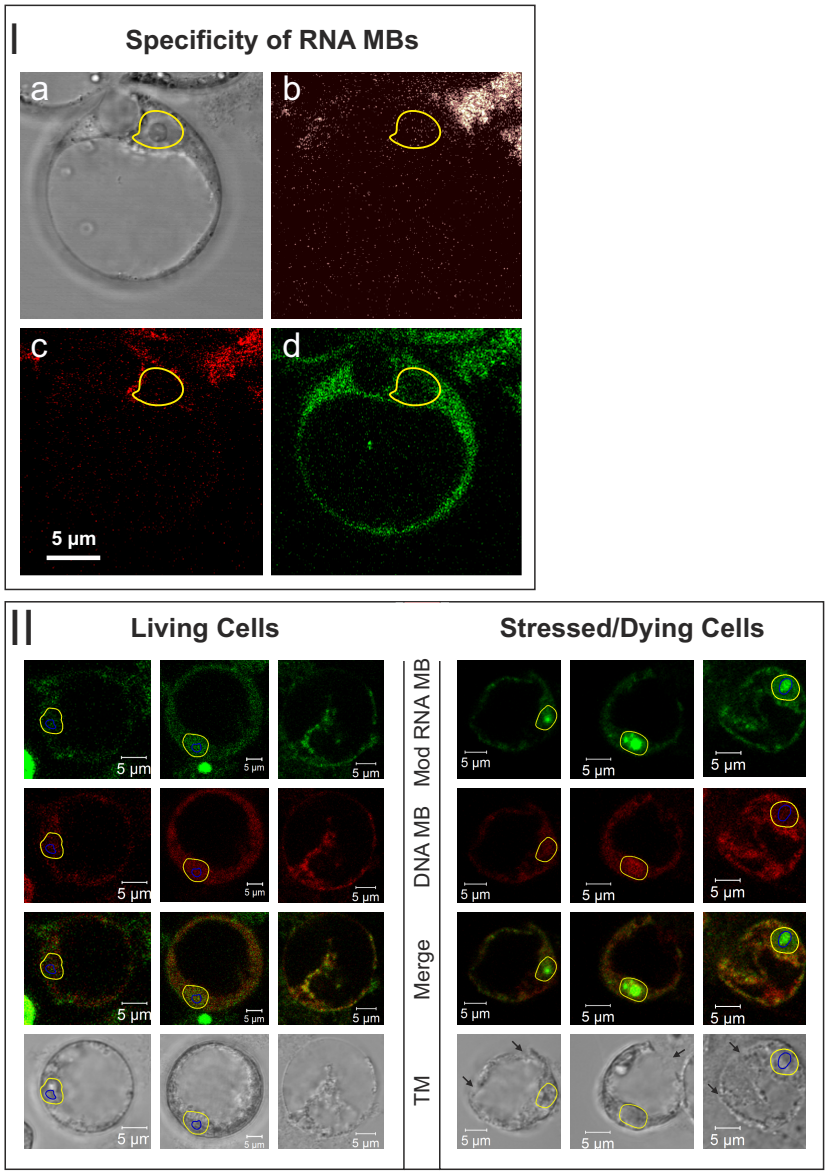

Supplemental Figure 2: I) Localization of 2'-O-methylated MBs in comparison with a scrambled DNA MB. Representative image of a protoplast transfected with a 2-O-methylated RNA MB labeled with an Atto550 fluorophore targeting exon 3 of the SEF factor (cells cotransfected with a FAM labeled scrambled DNA MB). a) Transmission image with visible nucleus (marked yellow). b) Cell autofluorescence at 633 nm illumination. c) The scrambled DNA MB signal. d) The specific 2-O-methylated MB signal targeting exon 3. II) Localization of 2'-O-methylated RNA MBs in comparison with an DNA MB (same sequence). Image of protoplasts cotransfected with a 2O-methylated RNA MB labeled with an Atto550 fluorophore and a DNA MB with an Atto647N fluorophore both targeting exon 3 of the SEF factor. Green channel: 2O-methylated RNA MB; Red channel: DNA MB; Merge of the two channels; Transmission image (nucleus yellow, nucleolus blue). The panel shows 3 examples for living cells and 3 examples for stressed or dying cells. Black arrows indicate holes within the cellular membrane. The nuclear and the prominent nucleolar accumulation of the 2O-methylated RNA MBs is clearly visible within dying cells, whereas this localization is not observable for the DNA MBs. Healthy and transfected cells show similar distribution of the 2O-methylated RNA MB and the DNA MB.

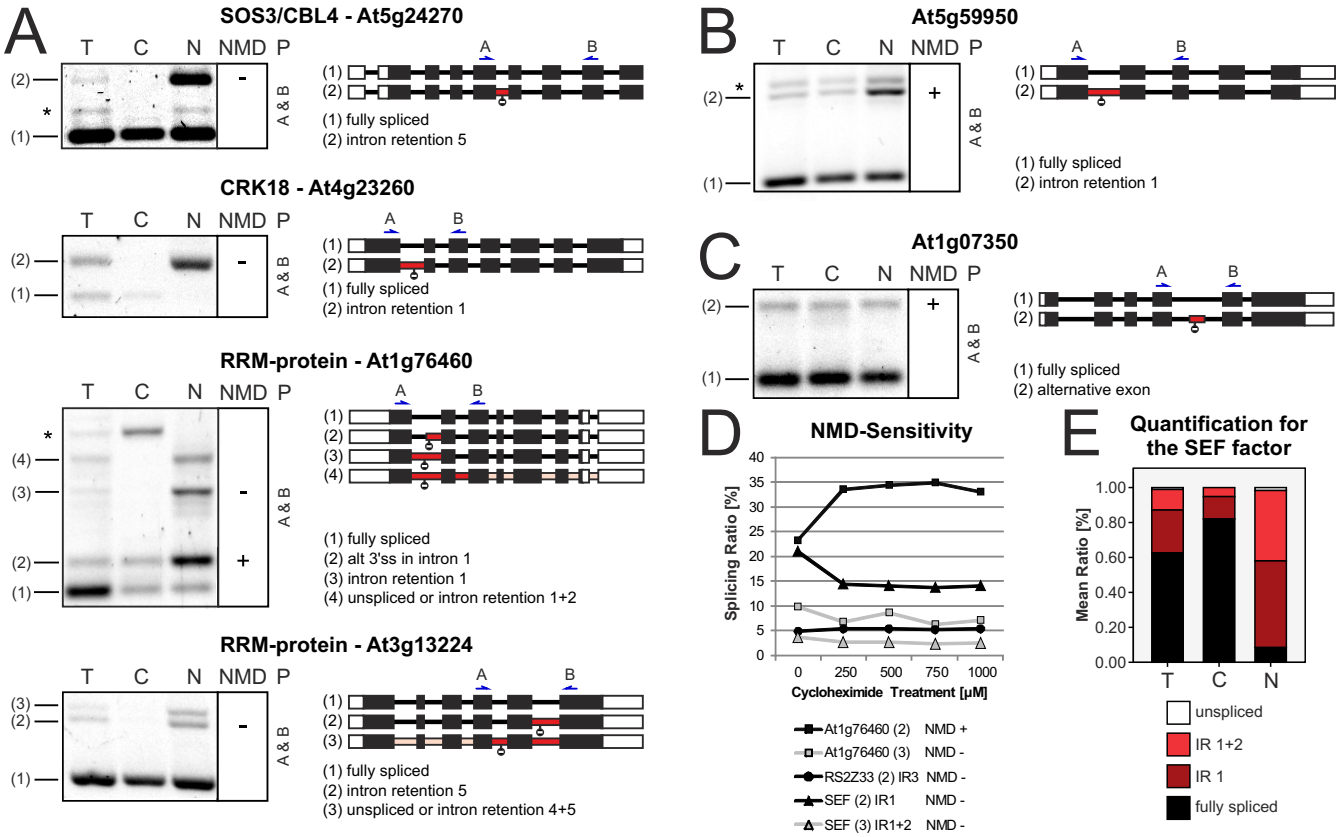

Supplemental Figure 3: Splice variants carrying NMD-negative but PTC+ intron retentions are present within the nuclear fraction. A) Gel-separation of RT-PCR products of At5g24270, At4g23260, At1g76460 and At3g13224 in fractionated cell extracts using the indicated primer pairs A&B. All tested NMD-negative transcripts with intron retention events are present within the nuclear fraction. However, NMD-positive transcripts as the alternative mRNA with 3'ss in intron1 of At1g76460 are also present within the cytoplasm. Stop signs indicate the position of the PTCs. B) Gel-separation of RT-PCR products of At5g59950 in fractionated cell extracts using the indicated primer pair A&B. The second transcript is the only known NMD-positive intron retention event and is present within the cytoplasm as well the as nucleus. C) Gel-separation of RT-PCR products of At1g07350 in fractionated cell extracts using the indicated primer pair A&B. The second transcript is a typical NMD-positive transcript present within the cytoplasm as well as the nucleus. D) Quantitative analysis of one NMD-sensitive splice variant and four NMD-insensitive splice variants upon treatment with a rising concentration of cycloheximide (inhibitor of NMD, $9e^{06}$ protoplasts were incubated in the dark at RT for 4h, 2 biological replicates, 2 technical reproductions). The experiment included gel-separation of the RT-PCR products of each investigated gene [oligo-dT oligonucleotides] and a subsequent quantitative gel analysis of the splicing ratios via ImageJ. The positive control increases from 23% to approximately 35%, whereas all tested NMD-insensitive splice variants did not accumulate. E) A quantitative analysis of the respective gel of the SEF factor. Quantification was performed via TotalLab Quant program. Each band was normalized to the total lane signal, yielding the ratio of a splice-variant per fraction. alt 3'ss -alternative 3' splice sites, T - total fraction, C - cytoplasmic fraction, N - nuclear fraction, NMD - indicates the sensitivity to the nonsense-mediated decay, P - primer pair, IR - intron retention, black boxes - exons, white boxes - untranslated regions, red - retained intronic sequences.

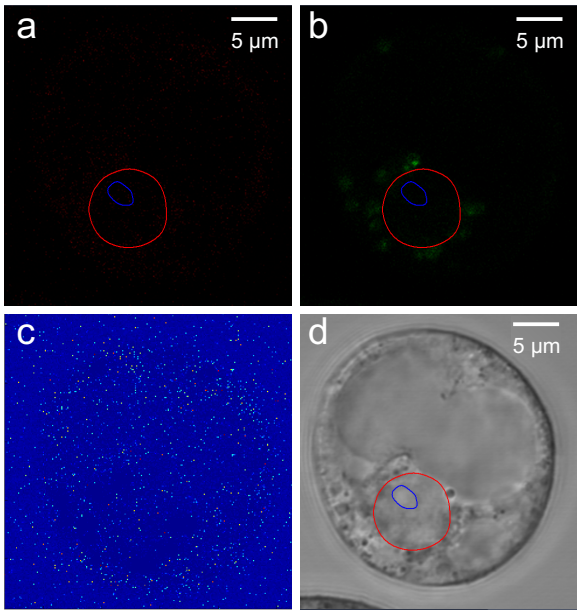

Supplemental Figure 4: The autofluorescence of wild type cells in the relevant channels. A representative image of a protoplast transfected with water. a) Autofluorescence at excitation of 561 (emission filters at 566-635). b) Autofluorescence at excitation 488 nm illumination (emission filters at 492-570). Autofluorescence is detectable within the perinuclear region, probable arising from plastid accumulation. c) Ratiometric image. d) Transmission image with visible nucleus (marked red) and nucleolus (marked blue).

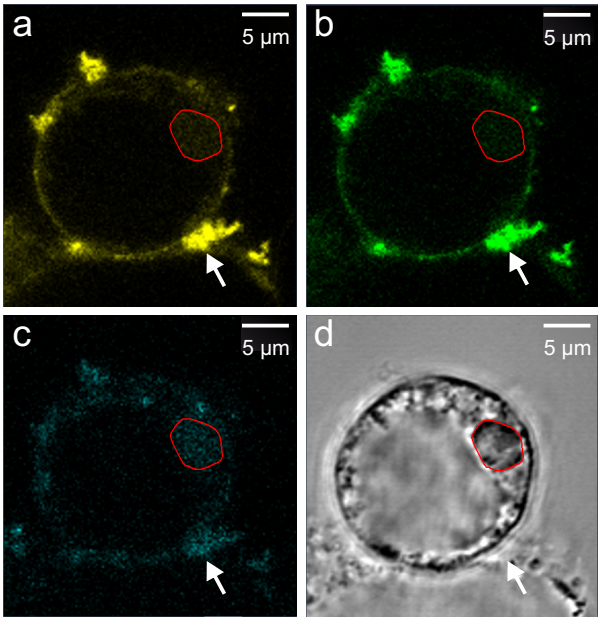

Supplemental Figure 5: Distribution of MBs within transfected cells. Shown is the localization of a dual-labeled MB (FAM at the 3end and Atto550 at the 5 end) targeting exon 3 of the SEF factor within a representative protoplast (uninduced RS2Z33 overexpresser line). a) The Att0550 signal (i.e. 561nm illumination, filters at 566-635). b) The FAM signal (488nm illumination, filters at 492-570). c) The FRET signal (488nm illumination, filters at 577-635). d) Transmission white light image with visible nucleus (marked red). The arrows mark extracellular debris.

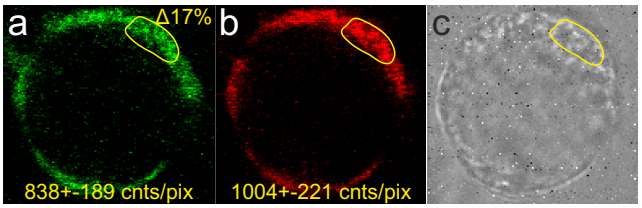

Supplemental Figure 6: Correction for quenching efficiency and quantum yields. a) Fluorescence image of the FAM/BHQ1-labeled MB after the correction of the excitation. b) Image of the Atto555/BHQ2-labeled MB. The image in a) is 17% darker than b), this corresponds to the difference in quenching efficiencies and quantum yields.

Supplemental Table 1. GO Biological Process classification of genes with NMD-insensitive IR events

gene	GO Biological Process
At5g37055	Chromatin remodeling defense response to bacterium regulation of developmental growth regulation of flower development
AT4G23260	maltose metabolic process response to abscisic acid stimulus starch biosynthetic process
At5g24270	calcium-mediated signaling cellular potassium ion homeostasis detection of calcium ion hypotonic salinity response stomatal movement
AT3G13224	NA
At1g76460	photoperiodism, flowering
AT2G28550	organ morphogenesis regulation of transcription, DNA -dependent response to abscisic acid stimulus response to salt stress vegetative to reproductive phase transition of meristem
At3g16800	NA
At5g13790	callose deposition in cell wall cellular membrane fusion cellular response to auxin stimulus embryo development ending in seed dormancy fruit abscission fruit dehiscence gibberellin catabolic process microsporogenesis negative regulation of floral organ abscission negative regulation of flower development negative regulation of seed maturation negative regulation of short-day photoperiodism, flowering ovule development positive regulation of transcription, DNA -dependent somatic embryogenesis negative regulation of transcription
At5g25610	response to abscisic acid stimulus response to cold response to desiccation response to salt stress
At1g49730	NA
At4g27410	abscisic acid mediated signaling pathway hyperosmotic salinity response positive regulation of transcription, DNA -dependent response to abscisic acid stimulus response to auxin stimulus response to cold response to ethylene stimulus response to jasmonic acid stimulus response to water deprivation response to wounding signal transduction

Supplemental Table 2. Sequences of the oligonucleotides and Molecular Beacons.

Oligonucleotide sequences used for RT-PCR

Name	Sequence
RS2Z33-exon 5 rev	5'-TAGCTTCGGCTACGGCTAAGACTC-3'
RS2Z33-exon 2 fw	5'-GACAATGCCTCGCTATGATGATCG-3'
RS2Z33-alt 3'ss fw	5'-CTTTTTAGCAGATACGGAAGGTCTC-3'
RS2Z33-intron 3 rev	5'-GGACAAAAGAGACCACATGCATGG-3'
SEF_exon 1 fw	5'-GGAAGAGATGTCGAACCGTCG-3'
SEF_exon 4 rev	5'-GCTGCTTTCAAGTAAGTCGG-3'
At1g07350	5'-CCTTGTCCTGGACCCATGGAC-3'
	5'-CTCGAGCAGTTCTCAGCCCC-3'
At5g24270	5'-GAGTTTGGTGAATTTGTCCGG-3'
	5'-GGCAAAGTCATGTTCTTGATG-3'
At1g76460	5'-GGTCGATCCAAAGGATATGG-3'
	5'-GGAAGTGGTTGCTGATACGG-3'
AT4G23260	5'-GGGAAGTGTATCCCTTCTCTGG-3'
	5′-GATTTCTCTTCGTAGGATCAAAG-3'
AT3G13224	5'-GGGTGACTACCGTAAGAAGG-3'
	5′-GGCGCTAGTCCTGGGAAAA-3′
At5g59950	5'-CTGCTCCATACCAATCAGCC-3'
	5'-CCACTTCTATCAAAATGAAC-3'
pMDC7-RS2Z33-HA	5′-GACACGCTGAAGCTAGTCG-3′
	5′-GGTGATGGTGGTGGGCTCCC-3′

Sequences of the Molecular Beacons

Name	Sequence
33mRNA_EJ6	5′-GATCGCGCGTGATCGGCTGTAGCTTCGGCCGCGATC -3′
33alt_EJ	5′-GATCGCGCCCAGAGACCTTCCGTATCTGCCGCGATC -3′
33alt_intron	5′-GATCGCGCATGCATGGTGTGTTTTCCCACCGCGATC -3′
Cat3/1	5′-GATCGCGAGGACTGGCACGTTCGTGGACACGCGATC -3′
SEF_IR2	5′- GATCGCGCTACAGATTCACACACAGAGCCGCGATC -3′
SEF_IR3	5′- GATCGCGGCCTAGCCGCAAAATAGTTAGCGCGATC -3′
SEF_EJ1	5′- GATCGCGGCTATAGCAGCCTGAGTTCGACGCGATC -3′
SEF_exon3	5′- GATCGCGCGCTTTGATCCTTTGTGTTGCCGCGATC -3′
Scramble	5′- GTACGCGGATGCGCGTACGACGTCTGAGACGCGTAC-3′
Scramble2	5′- GGCGTACGAGCGGTAATTCTGGCAAGCGAGTACGCC-3′